VOLUME 111, NUMBER 15
JULY 19, 1989
© Copyright 1989 by the
American Chemical Society

JOURNAL
OF THE
AMERICAN
CHEMICAL
SOCIETY

Deep-Ultraviolet Raman Excitation Profiles and Vibronic Scattering Mechanisms of Phenylalanine, Tyrosine, and Tryptophan

Stephen P. A. Fodor, Robert A. Copeland, Christine A. Grygon, and Thomas G. Spiro*

Contribution from the Department of Chemistry, Princeton University, Princeton, New Jersey 08544. *Received October 13, 1988*

Abstract: Raman cross sections for excitation at wavelengths between 240 and 192 nm have been determined for resonance-enhanced ring modes of phenylalanine (Phe), tyrosine (Tyr), tyrosinate (Tyr^-), and tryptophan (Trp) and for the breathing mode of SO_4^{2-} and the symmetric OH stretching mode of H_2O. The SO_4^{2-} and H_2O bands, which are frequently used for relative intensity measurements, show strong preresonance enhancement at wavelengths below 220 nm, requiring large corrections to convert relative to absolute intensities. The aromatic amino acid intensity measurements were obtained with laser power levels in the linear regime and appear not to be influenced by saturation effects or photochemical transients. The 1210-cm^{-1} ring–C stretching mode of Phe and Tyr and the ring modes ν_{12} (Phe, 1000 cm^{-1}) or ν_1 (Tyr, 850 cm^{-1}) show strong enhancement in resonance with the allowed $B_{a,b}$ transition and weak enhancement in resonance with the quasi-forbidden L_a transition. Their excitation profiles (EPs) peak on the red side of the L_a absorption band, consistent with destructive interference between L_a and $B_{a,b}$ contributions to the *A*-term Raman amplitude. The modes ν_{8a}, ν_{8b} ($\sim$1610, 1590 cm^{-1}), and ν_{9a} ($\sim$1180 cm^{-1}), known to be responsible for the vibronic intensity of the L_a transition, are resonant with the L_a transition but also with the $B_{a,b}$ transition. Enhancement of ν_{8b}, which is antisymmetric in the molecular C_{2v} symmetry, requires *B*-term activity for the $B_{a,b}$ as well as the L_a states. The $B_{a,b}$ enhancement (192-nm excitation) of ν_{8b}, as well as ν_{8a} and ν_{9a}, increases in the order Phe < Tyr < phenolate $\approx$ Tyr^-. This effect is suggested to arise from the substituent electronic perturbation, which leads to a B_a origin shift along ν_{8a} and ν_{9a} and vibronic mixing between B_a and B_b via ν_{8b}. In the L_a region the EPs of ν_{8a}, ν_{8b}, and ν_{9a} are skewed to the blue side of the L_a absorption band, for Tyr more than Phe, suggesting constructive L_a–$B_{a,b}$ interference for the *B* Raman terms. The Phe ν_{8a} and ν_{8b} overtones and combination bands are more strongly enhanced in resonance with $B_{a,b}$ than are the fundamentals; the $2\nu_{8a}/\nu_{8a}$ intensity ratio reaches a value of 2.1 at 192 nm. This effect is attributed to force constant changes in the allowed excited states. The $2\nu_{8a}$ cross section is much lower for Tyr but increases again for Tyr^-, although the fundamental band is now much stronger. Evidently the B_a force constant change is diminished by the OH substituent, while the increased origin shift for O^- increases the overtone intensity again. The Tyr $2\nu_{8b}$ cross sections are about half those of Phe and the $2\nu_{8b}/\nu_{8b}$ ratio, $\sim$0.15, is suggested to reflect the relative magnitude of *C* and *B* vibronic terms. Several Trp modes give EPs which track the strong 220-nm absorption band, attributed to B_b. These modes have significant five- and six-membered ring involvement, implying delocalized character for the transition. The benzene-like ν_{8a} and ν_{8b} modes are enhanced in the short-wavelength absorption band ($\sim$195 nm), attributed to B_a. The ν_{8a} mode is also weakly resonant with the B_b, indicating some displacement of the excited state along the ν_{8a} coordinate. The ν_{8b} mode, however, is not enhanced in the 220-nm band; this behavior can be understood on the basis of the ν_{8b} eigenvector being essentially antisymmetric to the polarization axis and therefore unable to support *A*-term activity in the B_b transition.

It has recently become possible to obtain Raman spectra with excitation in the deep-ultraviolet region[1-5] and thereby study resonance effects in simple conjugated molecules. This development greatly expands the applicability of Raman spectroscopy in the study of biomolecules since nucleic acid bases, aromatic side chains of amino acids, and the peptide bond itself all have

* Author to whom correspondence should be addressed.

(1) Ziegler, L. D.; Hudson, B. S. *J. Chem. Phys.* **1981**, *74*, 982.
(2) Ziegler, L. D.; Hudson, B. S. *J. Chem. Phys.* **1983**, *79*, 1134.
(3) Rava, R. P.; Spiro, T. G. *J. Am. Chem. Soc.* **1984**, *106*, 4062.

0002-7863/89/1511-5509$01.50/0 © 1989 American Chemical Society

electronic transitions in the ultraviolet region, and their structures can now be studied by UV resonance Raman (UVRR) spectroscopy.

In their pioneering UVRR study utilizing the YAG laser fifth harmonic at 213 nm, Ziegler and Hudson elucidated the resonance Raman mechanisms of benzene[1] and alkylbenzenes,[2] parent chromophores for the aromatic amino acids phenylalanine, tyrosine, and tryptophan, whose UVRR characteristics were described by Rava and Spiro,[3,6] using excitation at 266, 240, 218, and 200 nm. It is important to determine the excitation wavelength dependence of these spectra in some detail, in order to understand the resonance-scattering behavior of the chromophores, and to determine optimum conditions for structural applications of UVRR spectroscopy. Recently Asher and co-workers[7] have utilized a YAG dye laser system to measure absolute Raman intensities for these molecules at wavelengths down to 220 nm. In the present study we use several H_2 Raman-shifted YAG laser lines for absolute intensity measurements at wavelengths down to 192 nm. The resulting excitation profiles reveal a number of novel features involving the interplay of vibronic and Franck–Condon activity for ring modes of the aromatic chromophores.

The intensities were determined at laser power levels low enough to avoid saturation or phototransient effects, which were a problem for Asher et al.,[7] preventing them from obtaining accurate profiles for tryptophan. We also report absolute intensity measurements for SO_4^{2-} and H_2O, which reveal significant preresonance enhancement factors at wavelengths below 220 nm. These factors become important when assessing relative intensity measurements using the SO_4^{2-} or H_2O bands as internal standards.

Experimental Section

Phenylalanine (Phe), tyrosine (Tyr), and tryptophan (Trp) were purchased from Sigma. Solutions of these amino acids (1 mM) were prepared in 0.05 M phosphate buffer (pH 7.0) containing 0.4 M sodium sulfate (added as an internal standard for Raman spectra). Reagent grade phenol was purified by distillation. Tyrosinate (Tyr^-) and phenolate solutions were prepared by raising the pH of Tyr and phenol solutions to 12.0, with NaOH. For excitation at 240 nm, solutions of Tyr and Phe were prepared at a concentration of 5 mM, and a neutral density filter was used to attenuate the laser power before the sample to avoid laser saturation effects on the Raman spectra.[8] The final concentrations of all species in solution were determined spectrophotometrically in the 200–300-nm region by using the extinction coefficients listed in Table II. UV absorption spectra were obtained with a Cary 118 UV–vis spectrophotometer that was flushed with N_2 for ~5 h before data acquisition. Samples were contained in 0.1-cm fused silica cells and were run with the appropriate buffer in the reference cell.

Raman spectra were obtained with excitation wavelengths from 240 to 192 nm produced by H_2-shifting of the frequency-doubled (532 nm), -tripled (355 nm), and -quadrupled (266 nm) output of a Nd:YAG laser, as described elsewhere.[5] Spectra were signal averaged over 5–10 scans.

Raman intensities, expressed as cross sections, σ, were determined from the peak height ratio, I_N/I_S, of the sample (N) and internal standard (S) vibrational bands by using

$$\sigma_N = \sigma_S(I_N/I_S)[(\nu_0 - \nu_S)/(\nu_0 - \nu_N)]^4(C_S/C_N) \quad (1)$$

where C_S/C_N is the concentration ratio, ν_0 is the laser excitation frequency, and ν_N and ν_S are the vibrational frequencies (Δ cm^{-1}) of the sample and standard Raman bands. Strictly speaking, the cross sections should be determined from peak areas, rather than heights, but the bandwidths are independent of the excitation wavelength. Polarization differences also influence the cross sections; the numbers obtained in this study represent the sum of scattering contributions parallel and perpendicular to the incident laser polarization, as no polarization analyzer was employed. The manufacturers' response curves for the spectrometer gratings (3600 groves/mm, holographic) showed minimal polarization dispersion. The possibility of polarization artifacts was checked by recording spectra of Phe and Tyr at all wavelengths with and without a quartz polarization scrambler (Airtron) suitable for the deep-UV region. Cross section differences with and without the scrambler were negligible. The scrambler was not used for Tyr^- or Trp to avoid saturation effects (see below) at the higher laser power necessitated by the scrambler.

Cross sections, σ_S, were determined for the 981-cm^{-1} ν_1 band of sulfate, by comparing the Rayleigh scattering intensity of standard $BaSO_4$ particles, as described by Dudik et al.[9] The 3450-cm^{-1} band intensity of H_2O was measured relative to sulfate by using the spectrum of aqueous Na_2SO_4. Sulfate was used as internal standard for all of the aromatic amino acid measurements; the value of σ_{SO_4} used in eq 1 was determined from a curve that best fit the experimental values as a function of wavelength (eq 2, next section). Intensities for the ν_{8a} and ν_{8b} overtones of Phe, Tyr, and Tyr^- were measured in D_2O, to avoid interference from the broad O–H stretching band of H_2O. The large frequency separation, relative to the fundamentals, as well as the sulfate internal reference, made it important to gauge the self-absorption and chromatic aberration corrections.[12] This was done by measuring the band intensities relative to nearby ethanol bands in a 1:1 D_2O/ethanol solution. The relative intensities of the ethanol bands were then compared with the ratio in pure ethanol, to obtain the required correction. The corrections were small for Phe and Tyr but substantial for Tyr^-, up to 50%, depending on the wavelength, because of the strong absorption due to hydroxide.

Table I. Absolute Intensities[a] for the 981-cm^{-1} ν_1 Band of Aqueous SO_4^{2-} and the 3450-cm^{-1} ν_{O-H} Band of H_2O

exc wavelength, nm	$\sigma(SO_4^{2-})$[a]	$\sigma(H_2O)$	exc wavelength, nm	$\sigma(SO_4^{2-})$[a]	$\sigma(H_2O)$
192	3.03	1.82	240	0.28	0.04
200	1.74	0.88	252	0.20	
209	1.04		266	0.13	0.01
218	0.67	0.21	282	0.09	
223	0.54		299	0.06	
229	0.42				

[a] Expressed in units of cross section, millibarns/(molecule steradian); 1 barn = 10^{-24} cm^2.

Results

Internal Standards: SO_4^{2-} and H_2O. Raman intensities are usually measured relative to a reference band of an internal standard present in the sample and can be converted to an absolute scale if the absolute intensity of the reference band is known. Even if this conversion is not made, the relative intensities can be used for plotting excitation profiles, provided that the reference band (which automatically contains the normal ν^4 excitation frequency dependence) is not itself subject to resonance effects in the region of interest. UVRR studies have generally employed as reference the ν_1 bands of the oxy anions SO_4^{2-}, ClO_4^- or PO_4^{3-} or the OH stretching mode of solvent H_2O. The latter has the advantage that no reference substance need be added to an aqueous sample. It has the disadvantage that its frequency, ~3450 cm^{-1}, is much farther from the RR bands that are generally of interest than are the oxy anion bands (~1000 cm^{-1}) and the relative intensity measurement is therefore subject to a larger correction for self-absorption.[5b] For SO_4^{2-}, ClO_4^-, NO_3^-, and CH_3CN the intensity variation with excitation wavelengths above 220 nm has been determined by Dudik et al.[9] We have now determined absolute intensities for SO_4^{2-} and also the H_2O bands at wavelengths between 300 and 192 nm. The results are given in Table I and plotted in Figure 1. We used the $BaSO_4$ diffuse scattering method introduced by Dudik et al.[9] and scaled our SO_4^{2-} σ_N value to theirs (which was in turn scaled to the known absolute intensity of benzene), measured at 282 nm. At 218 nm, the other wavelength common to both studies, the disagreement between the two σ_S values was <10%. The σ_N values for H_2O, determined for the same Na_2SO_4 solution, was scaled to the SO_4^{2-} values. Below 220 nm intensities for both SO_4^{2-} and H_2O increase sharply, reflecting incipient resonance with deep-UV electronic transitions. In both cases there is a factor of ~10 increase between 220 and 192 nm. Thus the wavelength variation for these reference bands

(4) Asher, S. A.; Johnson, C. R.; Murtaugh, J. *Rev. Sci. Instrum.* **1983**, *454*, 1657.
(5) (a) Fodor, S. P. A.; Rava, R. P.; Copeland, R. A.; Spiro, T. G. *J. Raman Spectrosc.* **1986**, *17*, 471. (b) Fodor, S. P. A.; Rava, R. P.; Hays, T. R.; Spiro, T. G. *J. Am. Chem. Soc.* **1985**, *107*, 1520.
(6) Rava, R. P.; Spiro, T. G. *J. Phys. Chem.* **1985**, *89*, 1856.
(7) (a) Asher, S. A.; Ludwig, M.; Johnson, C. R. *J. Am. Chem. Soc.* **1986**, *108*, 3186. (b) Ludwig, M.; Asher, S. A. *J. Am. Chem. Soc.* **1988**, *110*, 1005.
(8) Johnson, C. R.; Ludwig, M.; Asher, S. A. *J. Am. Chem. Soc.* **1986**, *108*, 905.
(9) Dudik, J. M.; Johnson, C. R.; Asher, S. A. *J. Chem. Phys.* **1985**, *82*, 1732.

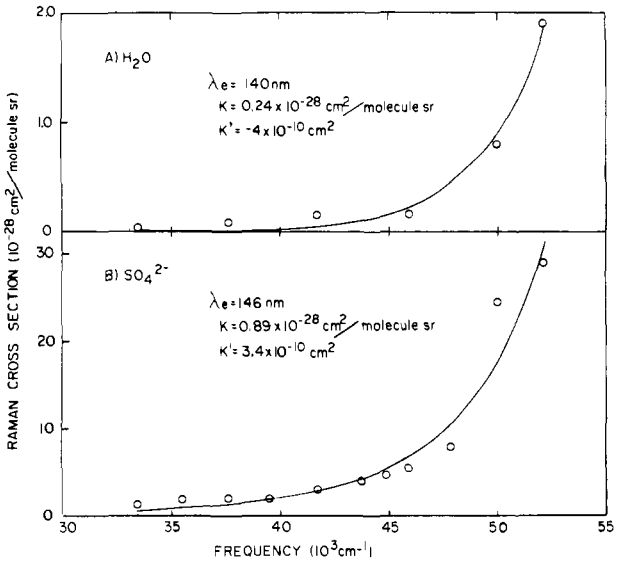

Figure 1. Absolute intensities for (A) the ν_{O-H} band (3450 cm^{-1}) of H_2O and (B) the ν_1 band (981 cm^{-1}) of SO_4^{2-} in aqueous Na_2SO_4 solution as a function of the excitation frequency. The solid lines are predicted frequency dependencies for *A*-term preresonance behavior (eq 2) for the indicated fitting parameters.

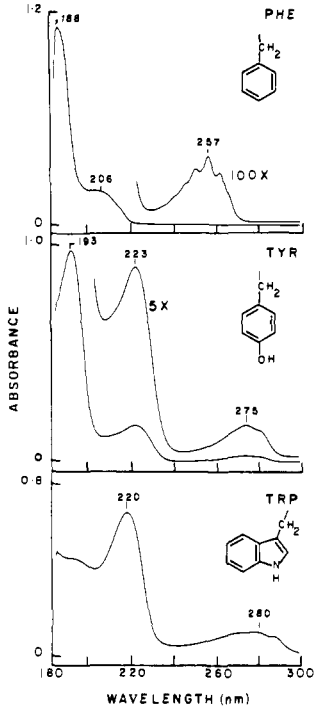

Figure 2. UV absorption spectra for phenylalanine, tyrosine, and tryptophan in aqueous solution; the side-chain molecular structures are shown.

is a significant factor for intensity measurements near 200 nm.

The solid curves in Figure 1 are fits to the data for preresonance enhancement via the *A* term in the Raman scattering equation[9]

$$\sigma_N = K\nu_0(\nu_0 - \nu_N)^3\left[\frac{\nu_e^2 + \nu_0^2}{(\nu_e^2 - \nu_0^2)^2} + K'\right]^2 \quad (2)$$

where K is a factor containing the Franck–Condon overlap in the resonant excited state, while ν_e is the frequency of the resonant electronic transition, ν_0 is the laser frequency, and ν_N is the frequency of the Raman transition. K' is a phenomenological parameter representing the off-resonant contributions of higher lying transitions, which flatten the curves at longer wavelengths. The best-fit wavelength, λ_e, for the resonant transition is 140 nm for H_2O and 146 nm for SO_4^{2-}. Both molecules show substantial absorption at wavelengths below 170 nm. Dudik et al.[9] obtained λ_e = 140 nm for SO_4^{2-}, in good agreement with our estimate, even though their data were limited to wavelengths above 220 nm. When K' was omitted from eq 2, however, their best-fit value decreased markedly, to 72.9 nm, whereas ours decreases only to 135 nm. The difference reflects the importance of the off-resonant contributions at longer wavelengths.

Table II. Absorption Maxima and Extinction Coefficients for the Aromatic Amino Acids and Model Compounds

molecule	transition		
	$B_{a,b}$	L_a	L_b
benzene[a]	183 (60)[b]	205 (7.4)	255 (0.3)
phenylalanine	188 (60.3)	206 (10.5)	257 (0.2)
phenol	188 (44)	210 (8.6)	268 (2.4)
tyrosine	193 (46.5)	223 (8.4)	275 (1.4)
phenolate	*c*	233 (9.4)	285 (2.6)
tyrosinate	*c*	240 (11.0)	293 (2.3)
tryptophan	218 (36.6)[d]	273 (6.0)[e]	287 (5.6)[e]

[a] Values taken from ref 23. [b] Numbers outside parentheses are wavelength maxima (nm) for the transitions while the values within parentheses are extinction coefficients (mM^{-1} cm^{-1}). [c] This region of the spectrum is obscured by hydroxide absorption. For tyrosinate, the ν_{8a}/ν_{8b} EPs suggest a maximum of ~195 nm (Figure 10, see text). [d] This band is assigned to a delocalized indole transition (see text). [e] Values taken from ref 4. Note that for tryptophan, the L_a and L_b transitions bands are unresolved.

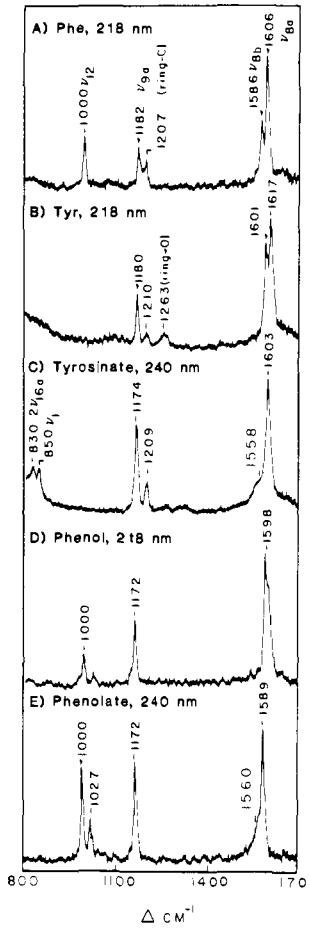

Figure 3. UVRR spectra of aqueous phenylalanine, tyrosine, tyrosinate (pH 12), phenol, and phenolate (pH 12) with excitation at 218 or 240 nm, in the L_a absorption bands. Note that ν_{8b} is strong for Phe, Tyr, and phenol but weak for tyrosinate and phenolate, suggesting dominant *B*-term activity for the former chromophores but *A*-term activity for the latter.

Aromatics. Figure 2 shows absorption spectra for phenylalanine (Phe), tyrosine (Tyr), and tryptophan (Trp), while Table II lists wavelength maxima and molar absorptivities for the first intense band, assigned to the benzene-like $B_{a,b}$ transition (except for Trp;

Table III. Raman Intensities (millibarns/(molecule steradian)) between 240 and 192 nm for the Prominent Ring Mode Fundamentals of the Aromatic Amino Acids

freq	assgnt[a]	σ_{192}[b]	σ_{200}	σ_{204}	σ_{209}	σ_{218}	σ_{223}	σ_{229}	σ_{240}
				Phenylalanine					
1000	ν_{12}	4970	236		68	176	51	11	10
1182	ν_{9a}	970	104	55	125	104	16	4	
1207	ring–C	3454	104	116	35	96	21	2	4
1586	ν_{8b}	632	236	362	266	187	25	1	
1606	ν_{8a}	632	261	451	463	366	52	11	6
				Tyrosine					
832	$2\nu_{16a}$	1022	325				46	48	8
852	ν_1	1869	814	190			64	65	10
1180	ν_{9a}	1208	606	349	215	197	210	206	20
1210	ring–C	4541	1406	334	82	41	58	77	9
1263	ring–O	3032	941	343	77	46	28		
1601	ν_{8b}	2255	1438	949	472	390	290	165	18
1617	ν_{8a}	4515	1879	1224	606	498	456	342	32
				Tryptophan					
762	W_{18}[c]	*e*	143	407	653	1301	996	356	18
880	W_{17}	*e*	71	119	221	455	398	122	6
1016	W_{16}	*e*	143	312	423	1445	1154	391	24
1127	W_{13}	*e*	135	208	183				6
1238	W_{10}	*e*	163	186	221	390	219	60	
1305	W_8	*e*	58	134	159	169	98		4
1342	*d*	*e*	156	277	284	273	329	113	16
1361	W_7	*e*	84	134	241	531	389	122	10
1462	W_5	*e*	105	186	159	311			8
1496	W_4	*e*	135	203	159	273			
1555	W_3	*e*	227	565	574	1558	937	292	22
1575	W_2	*e*	248	402	270				6
1622	W_1	*e*	242	350	270	48	288	99	32

[a] Assignments for phenylalanine and tyrosine from ref 6 and 18. [b] σ_i = Raman intensity at excitation wavelength i (nm). [c] Assignments for tryptophan from ref 18. [d] This band has been shown to be involved in a Fermi resonance interaction with W_7; the exact mode assignment is uncertain.[18] [e] The Raman intensity for tryptophan at 192 nm was too weak to be accurately measured.

Table IV. Far-UV Raman Intensities (millibarns/(molecule steradian)) for ν_{8a} and ν_{8b} Fundamentals, Overtones, and Combinations of Phenylalanine, Tyrosine, and Tyrosinate in D_2O Solution

	σ_{192}[a]	σ_{200}	σ_{204}	σ_{209}	σ_{218}
		Phenylalanine			
ν_{8a}	620	319	322	437	296
$2\nu_{8a}$	1292	542	373	250	68
ν_{8b}	688	251	219	265	155
$2\nu_{8b}$	662	369	173	131	33
$\nu_{8a} + \nu_{8b}$	1093	420	246	188	38
		Tyrosine			
ν_{8a}	4753	2420	884	528	321
$2\nu_{8a}$	*b*	*b*	55	32	25
ν_{8b}	2340	1371	575	413	192
$2\nu_{8b}$	*b*	209	100	95	31
		Tyrosinate			
ν_{8a}	1623	1908	1736	526	168
$2\nu_{8a}$	705	649	318	54	*b*
ν_{8b}	500	478	434	154	62
$2\nu_{8b}$	*b*	*b*	*b*	*b*	*b*

[a] σ_i = Raman intensity at excitation wavelength i (nm). [b] Signal too weak to measure.

see below) and the two lower energy weaker bands, assigned to the benzene-like L_a and L_b transitions; benzene, phenol, phenolate, and tyrosinate are also included in the table. Figures 3 and 4 compare UVRR spectra with excitation in resonance with the L_a band (218 or 240 nm) and the $B_{a,b}$ band (192 nm) for Phe, Tyr, and tyrosinate (Tyr^-) as well as phenol and phenolate. These illustrate interesting trends in the vibronic and/or Franck–Condon activity of ring modes as discussed below. Table III lists absolute intensities for selected modes of Phe, Tyr, and Trp for the eight laser wavelengths used in this study, while Figures 5–7 show plots of the resulting excitation profiles (EPs). Overtone intensities for the Phe, Tyr, and Tyr^- modes ν_{8a} and ν_{8b}, obtained in D_2O, are compared with the fundamental intensities in Table IV, while the EPs are shown in Figures 8–10. The spacing between the points

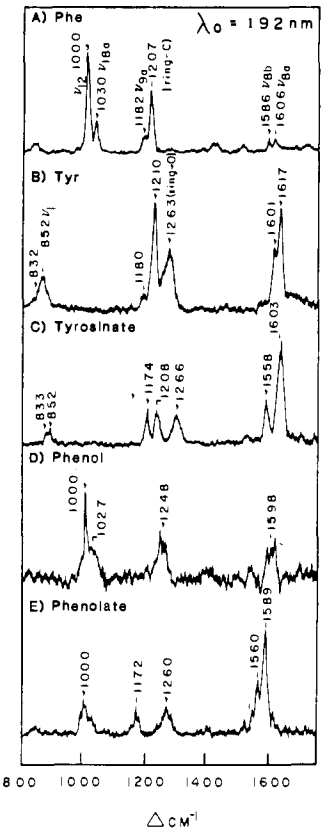

Figure 4. As in Figure 3, but with 192-nm excitation, in the $B_{a,b}$ absorption bands. Note that ν_{8a} *and* ν_{8b} increase intensity, relative to the ring breathing modes in the order Phe < phenol < Tyr < tyrosinate, phenolate (see text).

is relatively wide, and the detailed structures of the profiles are therefore uncertain. The available wavelengths are, however,

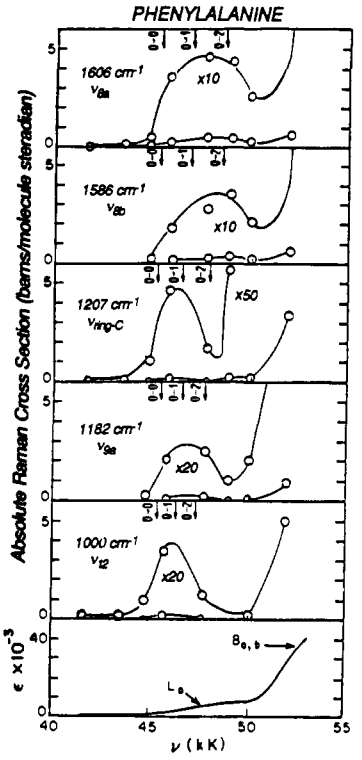

Figure 5. Excitation profiles (EPs) for prominent phenylalanine RR bands in the region of the L_a and $B_{a,b}$ absorption bands (bottom panel). Scale factors are shown for the amplified L_a region. The ν_{ring-C} and ν_{12} EPs are skewed to the red side of the broad L_a band, while the ν_{8a}, ν_{8b}, and ν_{9a} EPs are blue-shifted. The arrow marked 0–0 is at the position estimated for the L_a origin from the absorption band inflection. The 0–1 and 0–2 arrows were positioned by adding the ground-state frequency of the mode being monitored to the 0–0 frequency.

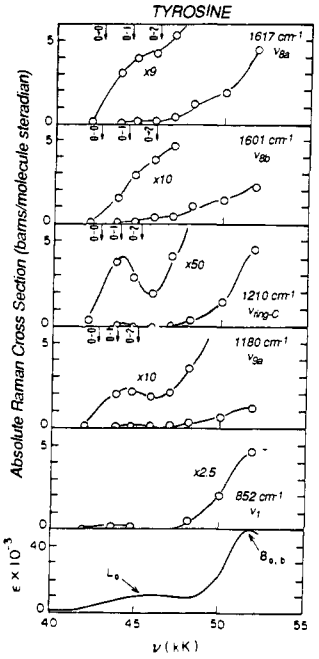

Figure 6. As in Figure 5, for tyrosine. Note the larger $B_{a,b}$ resonant enhancement of ν_{8a} and ν_{8b}, attributed to vibronic coupling of the split B_a and B_b components. The arrows were positioned as in Figure 5.

strategically located with respect to the electronic transitions of the chromophores under study, and the low-resolution profiles are quite informative with respect to the resonance enhancement mechanisms.

Figure 11 is a plot of intensity, relative to the SO_4^{2-} internal standard, for the 762-cm^{-1} band of tryptophan against incident laser power at 218 nm. Over a considerable range, the ratio is

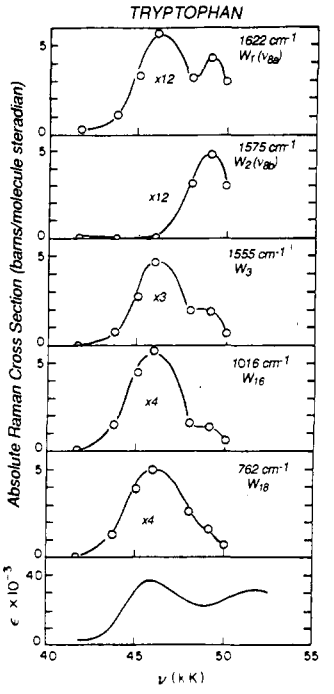

Figure 7. EPs for prominent tryptophan RR bands, scaled according to the indicated factors to facilitate comparison. All bands *except* W_2 (ν_{8b}) are resonant with the 218-nm absorption band, which is suggested to arise from an indole-delocalized transition, while only W_1 (ν_{8a}) and W_2 (ν_{8b}) are strongly resonant with a transition at ~202 nm, suggested to be analogous to the benzene $B_{a,b}$ transition.

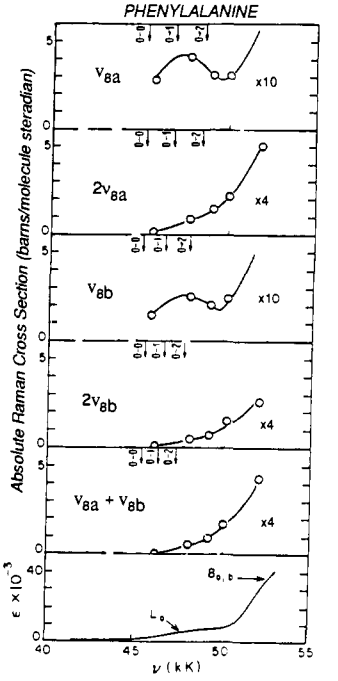

Figure 8. Comparison of phenylalanine far-UV EPs for the ν_{8a}/ν_{8b} fundamentals and overtone/combination bands, as well as the overtone/fundamental intensity ratios (inset).

constant, as expected if the sample and reference bands are both increasing linearly with laser power. At the highest power level, the relative intensity falls off, reflecting a significant pumping rate for the tryptophan excited state (saturation) and/or photochemical transformation of the tryptophan. We estimate the energy density at the laser focus to be ~160 mJ/cm^2 at the start of the nonlinear region. For tyrosine and phenylalanine, even higher power levels could be employed before nonlinear effects became significant. In all cases the reported intensities were obtained with the laser power in the linear regime.

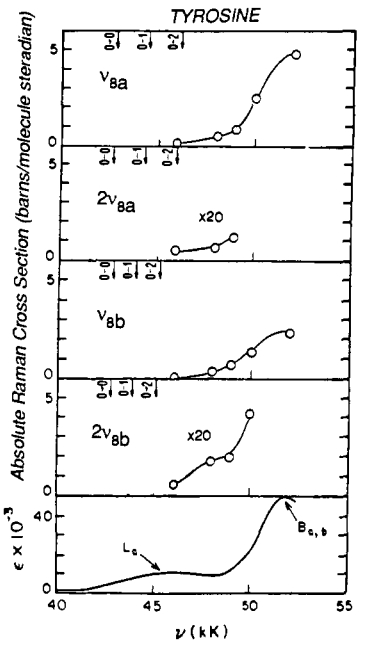

Figure 9. As in Figure 8, for tyrosine. The overtone intensities were too weak for measurement at the available signal/noise with 192- and (for ν_{8a}) 200-nm excitation. The $\nu_{8a} + \nu_{8b}$ combination band was not resolved.

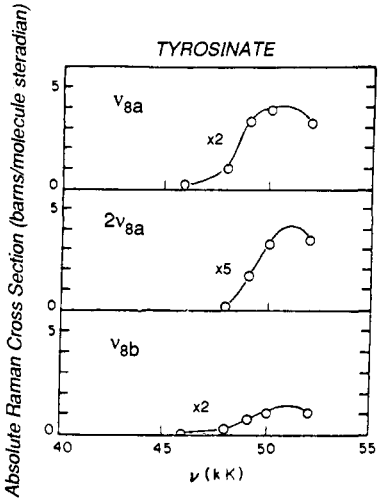

Figure 10. As in Figure 8, for tyrosinate. The $\nu_{8a} + \nu_{8b}$ combination band was not resolved.

Asher and co-workers first noted nonlinear intensity effects for Tyr and Trp[8] and discovered concurrent transient formation of tyrosyl and tryptophyl radicals during the intense laser pulses. Reexamination of the UVRR spectra of Rava and Spiro[3] shows detectable contributions of tyrosyl radical to the Tyr spectrum excited at 240 nm but not at 218 or 200 nm. We surmise that radical formation is more likely with 240-nm excitation because high laser powers are required to overcome the relatively low tyrosine enhancement at this wavelength. It may also be the case that the tyrosyl radical RR spectrum is less strongly enhanced at shorter wavelengths so that small amounts of radical would go undetected. It is important to check for a linear response to laser power in reporting RR intensities, which we have done in this study.

Asher et al.[7a] reported considerable difficulty with Trp intensity measurements, due to saturation and radical formation, and their tryptophan excitation profiles showed irregularities as a result. Likewise Tyr intensities were subject to saturation effects unless low laser powers were used.[7b] The Trp spectra of Rava and Spiro[3] show no radical peaks, and, as demonstrated in Figure 8, we were readily able to avoid nonlinear effects on the Trp intensities, as well as on Tyr and Phe intensities. We attribute the differences

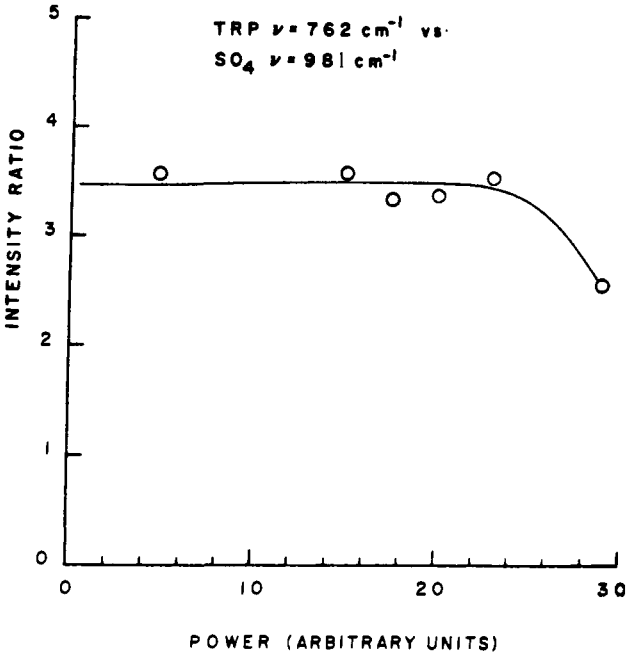

Figure 11. Relative intensity of the tryptophan 762-cm^{-1} band excited with 218-nm excitation as a function of laser power. The scale is arbitrary because the absolute pulse energy is unknown; relative power levels were set with calibrated neutral density filters.

between the two laboratories to our use of a single monochromator, with much higher throughput than the triple monochromator employed by Asher and co-workers.[4] The higher throughput means that we could obtain adequate signal/noise with less laser power and/or a less tightly focused beam.

Discussion

A. General Considerations. Benzene and Toluene. Near resonance with a transition to an electronic state, e, the Raman intensity[10,11] can be expressed in simplified notation as

$$I \propto |A + B + C|^2 \tag{3}$$

where

$$A = M_e^2 \hbar^{-1} \sum_v F_v/(\Delta\nu_v + i\Gamma_v); \quad F_v = \langle j|v\rangle\langle v|i\rangle \tag{4}$$

$$B = M_e M'_{e(Q)} \hbar^{-1} \sum_v F'_v/(\Delta\nu_v + i\Gamma_v); \quad F_v' = \langle j|Q|v\rangle\langle v|i\rangle + \langle j|v\rangle\langle v|Q|i\rangle \tag{5}$$

$$C = M'^2_{e(Q)} \hbar^{-1} \sum_v F_v''/(\Delta\nu + i\Gamma_v); \quad F_v'' = \langle j|Q|v\rangle\langle v|Q|i\rangle \tag{6}$$

For each term the resonance denominator is given by the detuning interval, $\Delta\nu_v = (\nu_{ev} - \nu_{gi}) - \nu_0$, where $\nu_{ev} - \nu_{gi}$ is the frequency separation between the vibrational level i of the ground state and the vibrational level v of the excited state, and ν_0 is the laser excitation frequency; to the detuning interval is added a damping factor $i\Gamma_v$, where Γ_v is the band width of the transition to ev. The A term depends on the square of the electric dipole transition moment, M_e, at the equilibrium geometry. M_e enters once for the upward and once for the downward virtual transition and is modified by the Franck–Condon overlaps $\langle v|i\rangle$ and $\langle j|v\rangle$, where i is the initial and j the final vibrational level. The fundamentals of nontotally symmetric vibrations ($i = 0, j = 1$) are not subject to A-term enhancement since they cannot displace the excited-state potential and consequently either $\langle j|v\rangle$ or $\langle v|i\rangle$ vanishes unless $j = i$ (Rayleigh scattering). However, their overtones and other

(10) Tang, J.; Albrecht, A. C. In *Raman Spectroscopy*; Szymanski, H. A., Ed.; Plenum: New York, 1970; Vol. II, pp 33–67.
(11) (a) Gerrity, D. P.; Ziegler, L. D.; Kelley, P. B.; Desiderio, R. A.; Hudson, B. *J. Chem. Phys.* **1985**, *83*, 3209. (b) Hudson, B. S.; Mayne, L. C. In *Biological Applications of Raman Spectroscopy*; Spiro, T. G., Ed.; Wiley: New York; Vol. II, Chapter 4, in press.

even harmonics ($i = 0, j = 2, 4, ...$) can be enhanced since $\langle 0|2\rangle$, $\langle 0|4\rangle$, etc., are nonzero provided there is a change in the force constant upon excitation, i.e., a change in the curvature of the excited-state potential. This situation is encountered for Phe, as discussed below.

The *B* term depends on the product of M_e and $M'_{e(Q)}$, the derivative of M_e with respect to displacement along the normal coordinate, Q, of the Raman transition. In this case the virtual transition, up or down, which is induced via $M'_{e(Q)}$, is modified by a Q-dependent vibrational integral $\langle v|Q|i\rangle$ or $\langle j|Q|i\rangle$. These integrals are nonzero for nontotally symmetric fundamental modes, whose appearance in resonance is a sure sign of *B*-term scattering. The *C* term depends on $M'^2_{e(Q)}$, both upward and downward virtual transitions being governed by the transition moment derivative, modified by a Q-dependent integral. Each of these integrals connects vibrational levels differing by one quantum, in the harmonic approximation. Consequently the product $F_v'' = \langle j|Q|v\rangle\langle v|Q|i\rangle$ is nonvanishing only for $j - i = 0$ (Rayleigh scattering) and $j - i = 2$, i.e., overtone scattering.

These equations are valid to the extent that M_e is a linear function of Q. They are written for a single normal mode, Q, but for a polyatomic molecule the overlap functions F_v, F_v', and F_v'' all contain Franck–Condon products $\langle i|v'\rangle\langle v'|i\rangle$ for normal modes along which the excited state is significantly displaced but which are not themselves excited in the Raman process being monitored. These multimode contributions to the intensity are important determinants of the enhancement factors and excitation profiles.[12] In addition, the Raman amplitudes should be summed over all the excited states, e. While the locally resonant state will ordinarily give the largest contribution, due to the energy denominator, interference effects are expected at excitation frequencies between electronic transitions.

For strongly allowed electronic transitions, $M_e \gg M'_{e(Q)}$, and the *A* term is the dominant scattering mechanism. For weakly allowed transitions it is possible that $M'_{e(Q)} > M_e$, in which case the *B* term is dominant. When the transition is electric dipole forbidden, $M_e = 0$, then both the *A* and *B* terms vanish, and only the *C* term survives, giving rise to overtone scattering (although enhancement of totally symmetric fundamentals is possible, via multimode effects[11]). The magnitude of $M'_{e(Q)}$ depends on the extent to which the vibrational coordinate Q is effective in coupling the resonant transition e with other (allowed) electronic transitions (Herzberg–Teller mixing[10]). The mixing modes are the ones that are subject to *B*- and *C*-term (vibronic) enhancement.

These considerations are nicely illustrated by the UVRR characteristics of benzene and alkylbenzenes, as elucidated by Ziegler and Hudson.[1,2] The first two electronic transitions of benzene, L_b (B_{2u}) and L_a (B_{1u}) are dipole forbidden by symmetry, while the third transition, $B_{a,b}$ (E_{1u}), is allowed. The L_a absorption band nevertheless has appreciable strength (Table II) because of vibronic mixing with the nearby $B_{a,b}$ transition, principally via the e_g ring modes ν_8 and, to a lesser extent, ν_9. Excitation at 213 nm, in resonance with L_a, produces enhancement of the overtone and combination bands of ν_8 and ν_9, via the *C* term.[1] Fundamental bands of ν_8 and ν_9 are not observed since the *A* and *B* terms are suppressed, M_e being zero. (Preresonance enhancement of these overtones (325-nm excitation) had earlier been reported by Ohta and Ito[13] and discussed in similar terms.) Enhancement is seen for the totally symmetric ring-breathing mode, ν_1, due to multimode effects. For toluene the electronic absorption spectrum is altered very little, but the methyl substituent breaks the D_{6h} molecular symmetry of benzene, and M_e is no longer zero. Indeed M_e and $M'_{e(Q)}$ now are inferred to be comparable since ν_8 and ν_9 fundamentals (split by the kinematic effects of the methyl group into ν_{8a}/ν_{8b} and ν_{9a}/ν_{9b} components) are about as strong in the 213-nm UVRR spectrum of toluene as are their overtones and combinations.[2]

B. Phenylalanine and Tyrosine. Phenylalanine is very similar to toluene in both its electronic (Figure 2) and vibrational spectrum, the toluene methyl substituent being replaced by the methylene group of an α-amino acid. The L_a-resonant (218 nm) fundamental region of the UVRR Phe spectrum is shown in Figure 3 and is essentially the same as that of toluene.[2] There is strong enhancement for ν_{8a}/ν_{8b} and moderate enhancement for ν_{9a}, the modes active in L_a–$B_{a,b}$ mixing. Also noticeable are the totally symmetric ring-C stretch at 1207 cm^{-1} and the ring mode ν_{12}, at 1000 cm^{-1}. (This mode has previously been labeled ν_1, by analogy with the benzene ring-breathing mode at 992 cm^{-1}, but as noted by Asher et al.,[7] the ring-breathing mode of Phe is lowered to 750 cm^{-1} via interaction with the ring-C stretch;[14] ν_{12} is also a radial mode, but alternating carbon atoms move toward and away from the center of the ring.) The ring-C stretch and ν_{12} probably gain their enhancement via the *A* term (see below). Asher et al.[7] have given a plausible rationale for a large origin shift of the L_a potential along the ν_{12} coordinate, based on a favorable match of the eigenvector with the B_{1u} orbital pattern of benzene. A similar argument was given for ν_{8a}, but as discussed in the next section the L_a-resonant activity of ν_{8a}, as well as ν_{8b}, is probably via the *B* term primarily.

The 218-nm UVRR spectrum of phenol (Figure 3) is nearly the same as that of phenylalanine (except that ν_{8a} and ν_{8b} are not clearly resolved). The ν_{12} intensity is somewhat lower for phenol and the ring–OH stretch, at 1248 cm^{-1}, is not observed. Likewise the UVRR spectrum of phenolate is similar when excited at 240 nm (Figure 3), taking into account the red-shift of the L_a absorption band (Table II). In this case ν_{12} is strong and another symmetric ring mode, ν_{18a} (1027 cm^{-1}), becomes noticeable. Finally tyrosine and tyrosinate show similar enhancement patterns for 218- and 240-nm excitation. Strong scattering is seen for ν_{8a}/ν_{8b} and ν_{9a}, while the totally symmetric ring–C and ring–O stretches are seen weakly. For these para-disubstituted benzenes, ν_{12} is not enhanced, but the ring-breathing mode ν_1, in Fermi resonance with $2\nu_{16a}$ to form the 850/830 cm^{-1} doublet,[15] can be seen (this feature is obscured in the Tyr spectrum by a rising background).

These similarities in the L_a-resonant behavior of all the mono- and para-disubstituted benzenes are in contrast with marked differences seen in the $B_{a,b}$-resonant UVRR (192 nm) spectra shown in Figure 4. For phenylalanine, the totally symmetric modes, ν_{12} and the ring–C stretch, dominate the spectrum, as expected for *A*-term enhancement via an allowed transition; the symmetric mode ν_{18a} is also prominent. In comparison, intensities are low for the modes ν_{8a}, ν_{8b}, and ν_{9a}, which are vibronically active in the L_a transition. By contrast ν_{8a} and ν_{8b} remain strong for tyrosine and especially for tyrosinate and phenolate; in the latter two cases even ν_{9a} is comparable in strength to the ring–C, ring–O, and ν_1 (or ν_{12}) modes. Phenol is an intermediate case with lower relative intensity of ν_{8a}/ν_{8b}, although still stronger than in phenylalanine.

We are thus required to explain how modes that are only vibronically activated in benzene become strongly enhanced in resonances with the allowed $B_{a,b}$ transitions when there is an OH or O^- substituent. Augmentation of ν_{8a}, which is a symmetric mode in the C_{2v} effective point group of these molecules, implies an increase in the Franck–Condon factor (*A* term). Since ν_{8a} derives from a nontotally symmetric benzene mode its Franck–Condon product is small if the perturbing effect of the substituent is slight, as is the case for CH_3. It is easy to see how more strongly perturbing substituents, OH and O^-, could increase the Franck–Condon product for ν_{8a}, which involves elongation of the ring in the direction of the substituent.[14]

The *A* term cannot account for ν_{8b} enhancement, however, since the eigenvector for this mode is antisymmetric with respect to the C_2 molecular axis. Although it is theoretically possible that the

(12) Myers, A. B.; Mathies, R. A. *Biological Applications of Raman Spectroscopy*; Spiro, T. G., Ed.; Wiley: New York; Vol. II, Chapter 2, in press.
(13) Ohta, N.; Ito, M. *Chem. Phys.* **1977**, *24*, 175.
(14) Dolish, F. R.; Fateley, W. G.; Bentley, F. F. *Characteristic Raman Frequencies of Organic Compounds*; Wiley: New York, 1974; pp 162–190.
(15) Siamwiza, M. N.; Lord, R. C.; Chen, M. C.; Takamatsu, T.; Harada, I.; Matsuura, H.; Shimanouchi, T. *Biochemistry* **1975**, *14*, 4870.

effective molecular symmetry is lower than C_{2v} for Phe and Tyr, due to unequal rotamer populations (with respect to rotation of the CH_2 and OH substituents) such an effect cannot explain ν_{8b} enhancement for phenolate ion, which has a single monoatomic substituent and rigorous C_{2v} symmetry. We therefore conclude that the enhancement of ν_{8b} implies *B*-term activity and propose that the states being mixed vibronically are B_b and the perturbed B_a. The unperturbed B_a and B_b wave functions do not mix vibronically. If they did, then Jahn–Teller activity would be observed in benzene; yet the ν_8 fundamental is unobserved in benzene RR spectra excited at wavelengths as short as 184 nm.[11a] But the perturbation of B_a by the OH and O^- substituents could induce B_a–B_b vibronic mixing.

An alternative view of the substituent effect is that the electronic perturbation mixes B_a with other electronic states, including the nearby L_a. Since ν_{8a} and ν_{8b} are vibronically active in the L_a state, mixing of L_a character into B_a could induce both Franck–Condon activity of ν_{8a} in B_a and B_a–B_b vibronic mixing via ν_{8b}.

Excitation Profiles for Phe and Tyr. Figure 5 shows absolute intensities for the major UVRR bands of Phe plotted against excitation frequency. In the L_a region the points are scaled up to reveal the gross structure of the profile. As noted above, the wavelength coverage is too coarse to be precise about the structure, and the lines connecting the points merely indicate the unresolved envelope. Nevertheless, it is apparent that the excitation profiles (EPs) fall into two classes, those for the vibronic modes ν_{8a}, ν_{8b}, and ν_{9a}, which are weakly enhanced via the $B_{a,b}$ transition (although their absolute intensities are actually slightly higher at 192 nm than in the L_a region), and the ν_{12} and ring–C modes, which are strongly $B_{a,b}$ resonant. In the L_a region the ν_{12} and ring–C EPs are relatively narrow, reaching a local maximum slightly to the blue of the expected L_a origin, ~46 000 cm^{-1}, where the absorption band has an inflection. In contrast ν_{8a}, ν_{8b}, and ν_{9a} show wide, blue-shifted EPs. Maximum enhancement is seen at wavelengths corresponding roughly to the 0–2 vibronic transition for the mode being monitored. (The estimated positions of the 0–0, 0–1, and 0–2 transitions of each vibration, by using the ground-state frequencies, are indicated by arrows in Figure 5.)

The difference in behavior of the two classes of EPs in the L_a region is attributed to predominant contributions from *B*- vs *A*-term mechanisms. The scattering amplitude for successive intermediate vibrational levels differ for the *A* and *B* term due to different magnitudes of the Franck–Condon and *Q*-dependent integrals. Moreover, interferences between successive vibronic or electronic states can differ because of different signs for these integrals. In the absence of interference effects the EPs are expected roughly to track the absorption band, as the ν_{8a}, ν_{8b}, and ν_{9a} EPs do. The shape of the ν_{12} and ring–C EPs suggest negative interference for the *A*-term scattering, leaving diminished intensity on the blue side of the absorption band. Negative *A*-term interference is expected if the origin shift of the L_a and B_a states (and therefore the signs of Franck–Condon factors) are in the same direction, since the detuning intervals, $\Delta\nu_v$, are opposite in sign for excitation between the states. A similar pattern is seen for tyrosine (Figure 6), the ν_{8a}, ν_{8b}, and ν_{9a} EPs being broader and shifted to the blue relative to the ring–C EP.

The tyrosinate EPs for ν_{8a} and ν_{8b} in the $B_{a,b}$ region (shown in Figure 10, where comparison is made with the overtone EPs; see below) show the $B_{a,b}$ transitions to be significantly red-shifted relative to tyrosine, both EPs peaking at ~200 nm. This red-shift cannot be seen in the absorption spectrum because of interference from OH^- in the solution. The absolute cross sections are significantly lower for Tyr^- than for Tyr. Interestingly, the L_a state is more red-shifted relative to Tyr (223 → 240 nm, Δ ~ 3200 cm^{-1}) than the $B_{a,b}$ state (193 → ~200 nm, Δ ~ 1800 cm^{-1}). The L_a state may have significant charge-transfer character in Tyr^-.[7] L_a-resonant EPs of Tyr^- have been reported by Asher et al.[7] for ν_{8a} and ν_{9a}. They are quite different from those seen for Tyr (Figure 6), showing clearly resolved 0–0 (~40 000 cm^{-1}) and 0–1 resonances, with only weak scattering at the 0–2 positions. No data were reported for ν_{8b}, which could not be resolved from ν_{8a} in the RR spectra. Actually the bands are well separated (45 cm^{-1}) as seen in Figure 4, but the L_a-resonant enhancement of ν_{8b} is relatively weak (see Figure 3) for Tyr^- in contrast to Tyr. This low enhancement of ν_{8b} implies that *B*-term activity is in this case less important than *A*-term activity for ν_{8a} (and ν_{9a}). Predominant *A*-term activity is also evident from the lower ν_{8a} and ν_{9a} enhancement, relative to Tyr, on the blue side of the Tyr^- L_a absorption band, consistent with the expected negative *A*-term interference. Thus, the strongly perturbing O^- substituent evidently mixes L_a with B_a sufficiently to produce dominant L_a-resonant *A*-term activity for ν_{8a} and ν_{9a}, via the augmentation of the L_a transition moment.

ν_{8a}/ν_{8b} Overtones of Phe, Tyr, and Tyr^-. In view of the prominence of the ν_8 overtones in UVRR spectra of benzene,[1,11] and toluene[2] we have determined their EPs for Phe, Tyr, and Tyr^- (Table IV). The data were collected from D_2O solutions to avoid interference with the overtones (~3200 cm^{-1}) from the H_2O stretching band. The intensities of the fundamentals are in reasonable but not exact agreement with those determined in H_2O (Table III). It is possible that there is a medium effect on the absorption strengths and RR intensities, due to the D/H isotope effect on the water H-bond network.

Figure 8 compares Phe EPs for $2\nu_{8a}$ and $2\nu_{8b}$, as well as $\nu_{8a} + \nu_{8b}$, with those of ν_{8a} and ν_{8b}, in the $B_{a,b}$ region. Interestingly, the overtone and combination intensities increase more strongly as the laser wavelength approaches the $B_{a,b}$ transitions than do the fundamentals. In the preresonance region, a more rapidly changing response of the overtones to excitation wavelengths is expected on theoretical grounds.[16] What is remarkable, however, is the extent of the overtone enhancement, relative to the fundamentals; at 192 nm $2\nu_{8a}$ is twice as strong as ν_{8a}. We were concerned that the overtone cross sections might be in error due to self-absorption and/or chromatic aberration effects and took the precaution of comparing the intensities with those of nearby ethanol bands in a 50:50 D_2O/ethanol mixture and referencing the ethanol intensity ratios to those measured in pure ethanol, as advocated by Myers and Mathies[12] (see Experimental Section).

The surprisingly large overtone/fundamental intensity ratios in resonance with the allowed $B_{a,b}$ transitions seem to require significant force constant changes in the resonant excited state. In this way nonzero even-quantum vibrational overlaps, $\langle 2|0\rangle$, $\langle 4|0\rangle$, etc., can be generated, allowing RR intensity for even harmonics (which are totally symmetric) via the *A* term. (We searched for the fourth harmonic, but it is evidently too weak to observe; no intensity was detectable at the third harmonic frequency, either, as expected.) Enhancement of the $\nu_{8a} + \nu_{8b}$ combination band also implies mixing of the ν_{8a} and ν_{8b} coordinates in the excited states.

Alternative explanations for the large overtone/fundamental intensity ratios are unreasonable. Thus, a large origin shift might lead to stronger overtone than fundamental scattering, via the *A* term, but strong third harmonic scattering would also be expected, contrary to observation, and in any event no origin shift is possible for the nontotally symmetric ν_{8b} mode. Stronger overtone than fundamental vibronic scattering can occur if the *C* term exceeds the *B* term, as happens in resonance with the L_a band of benzene[1,11a] or (sometimes) the *Q* band of metalloporphyrins.[17] But this requires that the transition moment be weaker than its derivative, $M_e < M'_e$, a condition that is excluded for an allowed transition.

It should be noted that Gerrity et al.[11a] considered whether $2\nu_8$ scattering in benzene arises from a force constant change in the E_{1u} ($B_{a,b}$) electronic state but rejected the possibility on the basis of the measured depolarization ratio, 0.41, with 213-nm excitation. This is close to the value expected for $B_{1u}(L_a)$–$E_{1u}(B_{a,b})$ vibronic coupling. Although the depolarization ratio does confirm the expected *C*-term enhancement in resonance with the B_{1u} state, it does not rule out additional enhancement in resonance with the E_{1u} state (183 nm). The depolarization ratio was not measured

(16) Ziegler, L. D.; Albrecht, A. C. *J. Raman Spectrosc.* **1979**, *8*, 73.
(17) Aramaki, S.; Hamaguchi, H.; Tasumi, M. *Chem. Phys. Lett.* **1983**, *96*, 555.

at shorter wavelengths. The 184-nm excited benzene RR spectrum[11a] did show strong $2\nu_8$ scattering, although in the absence of cross-section measurements it is impossible to be certain that the intensity arose from the E_{1u} rather than the B_{1u} state. Our excitation profiles show $2\nu_{8a}$, $2\nu_{8b}$, and $\nu_{8a} + \nu_{8b}$ of Phe to be resonant with the $B_{a,b}$ state. There is no evidence for a discrete L_a resonance as there is for the fundamentals (which peak at ~48 000 cm^{-1}) although a weak resonance merging with the stronger $B_{a,b}$ resonance cannot be ruled out.

The Tyr ν_{8a} and ν_{8b} and Tyr^- ν_{8a} overtones are also enhanced in resonance with the $B_{a,b}$ transitions (Figures 9 and 10), but the quantitative intensity relationships differ dramatically from Phe. Thus the $2\nu_{8a}$ cross sections are an order of magnitude lower for Tyr than Phe, and the $\nu_{8a} + \nu_{8b}$ combination cannot be resolved. It appears that the ν_{8a} force constant change in the B_a state as well as the $\nu_{8a} + \nu_{8b}$ coordinate mixing, are much lower for Tyr. This effect may be due to the same electronic mixing that is responsible for the stronger ν_{8a} and ν_{8b} fundamental scattering of Tyr than Phe (see above). The mixing may reduce the mode alteration in the B_a state while also increasing the origin shift along ν_{8a}. The origin shift remains modest, however, as seen in the small $2\nu_{8a}/\nu_{8a}$ intensity ratio, ~0.07. This ratio and the ν_{8a} intensity increase markedly for Tyr^-, consistent with more extensive B_a–L_a mixing and a larger origin shift. The fact that the ν_{8a} fundamental intensity is lower than for Tyr, despite a larger origin shift, suggests that the Tyr^- B_a transition moment is lower. This would again be consistent with stronger B_a–L_a mixing for Tyr^-, which would distribute the allowed transition intensity between the two states.

The $2\nu_{8b}$ cross sections for Tyr are about half the values seen for Phe. The Tyr $2\nu_{8b}/\nu_{8b}$ ratios are relatively small, ~0.18. Most likely they represent the ratio of *C* and *B* terms that arise from the B_a–B_b vibronic mixing. The Tyr^- $2\nu_{8b}$ was too weak to be detected.

Excitation Profiles for Tryptophan. Figure 7 shows EPs in the 240–200-nm region for the strong bands of tryptophan. Data have also been reported for this molecule by Asher et al.[7] at wavelengths down to 220 nm. Although their EPs show fluctuations associated with saturation effects, resonance with the strong electronic transition at 218 nm is evident for all bands except the one at 1555 cm^{-1} (which was not observed in the 220–240-nm region), in agreement with our EPs. (For unknown reasons the tryptophan vibrational frequencies reported by Asher et al. differ by 5–10 cm^{-1} from ours, although the phenylalanine and tyrosinate frequencies are in agreement.) Because the data of Asher et al. did not extend below 220 nm, their EPs do not show the intensity rise at 200 nm for the 1575- and 1622-cm^{-1} bands. This is the most interesting feature of the enhancement pattern and forms the basis of our analysis.

The absorption spectrum of tryptophan resembles those of the benzene derivatives (Figure 2) and has been interpreted in terms of red-shifted benzene-like transitions. The broad, relatively weak band at ~280 nm is thought to contain overlapping contributions from L_a and L_b; these have been assigned at 273 and 287 nm for aqueous solution spectra,[18a] while the L_b origin band was located at 283.8 nm in a supersonic jet spectrum.[18b] Excitation at 266[6] or 257 nm[19] produces RR spectra dominated by bands at 1622 and 1575 cm^{-1}, assigned by Rava and Spiro[6] to ν_{8a}- and ν_{8b}-like modes of the six-membered ring of indole. Asher et al.[7] preferred to assign the band at 1555 cm^{-1} to ν_{8a} and the 1575-cm^{-1} band to a pyrrole mode. However, the eigenvectors resulting from the recent normal coordinate analysis by Takeuchi and Harada[20b] leave little doubt that benzene-like ν_{8a} and ν_{8b} are apt designations for the 1622- and 1575-cm^{-1} bands (W1 and W2 modes). In particular the phasing of the benzene C–C stretches in the 1575-cm^{-1} mode is antisymmetric with respect to the pseudo-2-fold (long) axis of indole, confirming the b designation. L_a-resonant enhancement of ν_{8a} and ν_{8b} is entirely as expected by analogy with phenylalanine and tyrosine, and the prominence of these modes in the Trp RR spectra excited near 270 nm provides strong support for the L_a assignment in this region.[18a]

The B_a and B_b transitions of the indole ring are widely split. PPP-SCF calculations by Song and Kurtin[21] placed them at 196 and 208 nm, respectively, and Auer[22] assigned the 195 and 220 nm absorption bands to these transitions. The ν_{8a} EP shows maxima coincident with both of these bands, but the ν_{8b} EP shows only the short wavelength maximum. We associate the lack of enhancement in the 220-nm absorption band to the polarization of the B_b electronic transition, which is calculated to be close to the long axis of the indole ring. Since ν_{8b} is antisymmetric with respect to this axis, its origin shift in the B_b state must be small. In the limit of C_{2v} symmetry for the indole ring, *A*-term activity would vanish for the antisymmetric ν_{8b}.

The character of the RR bands which are strongly resonant with the 220-nm transition suggest that it is delocalized over the entire indole ring, consistent with the near-long axis polarization. Thus the 762-cm^{-1} (W_{18}) and 1016-cm^{-1} (W_{16}) modes are best described as in- and out-of-phase combinations of benzene and pyrrole breathing modes,[6,20] while the 1555-cm^{-1} band (W_3) is calculated[18] to be pyrrole C_2–C_3 stretching primarily. These modes are only weakly resonant with the shorter wavelength absorption band, which is selective for ν_{8a} and ν_{8b} enhancement, suggesting that the B_a transition is more localized on the benzene ring.

We note that Rava and Spiro[6] reported numerous bands in the 200-nm excited Trp RR spectrum and an order of magnitude loss in overall enhancement relative to excitation at 218 nm. They attributed this diminution and the distribution of intensity into many modes to breakdown of the Born–Oppenheimer approximation due to crowding of electronic transitions at higher energies. The intensity loss was, however, overestimated because the preresonance enhancement of the reference water band was unrecognized. The actual EPs (Figure 6) show the main intensity loss to be associated with 762-, 1016-, and 1555-cm^{-1} bands (factor of 5–6 between 218 and 200 nm), which are simply not strongly resonant with the ~200-nm transition. While the numerous comparable RR bands seen with 200-nm excitation may indeed reflect contributions from several excited states, there does not appear to be a compelling need to invoke Born–Oppenheimer breakdown.

Conclusions

1. UV excitation profiles for Phe and Tyr are consistent with weak L_a-resonant and strong $B_{a,b}$-resonant *A*-term activity for the ring breathing and ring–C stretching modes. The EPs peak near the L_a 0–0 wavelength and diminish in the blue region of the absorption band consistent with destructive L_a–$B_{a,b}$ interference, as expected for excited-state displacements of the same sign.

2. The vibronic mixing modes ν_{8a}, ν_{8b}, and ν_{9a} show $B_{a,b}$-resonant activity in the order Phe < phenol < Tyr < phenolate ≈ Tyr^-. This activity is attributed to substituent-induced electronic perturbation of the B_a state, leading to origin shifts of B_a along ν_{8a} and ν_{9a} and vibronic mixing of B_a with B_b via ν_{8b}. For Tyr^- the ν_{8a} EP in the L_a absorption band suggests dominant *A*-term activity, due to strong L_a–B_a mixing, which also produces stronger ν_{8a} overtone activity, relative to Tyr, in resonance with B_a.

3. The Phe $\nu_{8a,b}$ overtones and the combination band are strongly enhanced relative to the fundamentals in resonance with the $B_{a,b}$ transitions; the $2\nu_{8a}/\nu_{8a}$ intensity ratio reaches 2.1 with 192-nm excitation. This activity seems to require force constant changes, as well as ν_{8a}–ν_{8b} coordinate mixing, in the $B_{a,b}$ states. The effect is greatly diminished in Tyr, whose ν_{8a} overtone intensities are an order of magnitude weaker. The substituent-induced B_a perturbation is suggested to reduce the force constant change and coordinate mixing. The Tyr ν_{8b} overtone activity is about half that of Phe, but the $2\nu_{8b}/\nu_{8b}$ ratio is relatively small

(18) (a) Yamamoto, Y.; Tanaka, J. *Bull. Chem. Soc. Jpn.* **1972**, *45*, 1362. (b) Bersohn, R.; Even, U.; Jortner, J. *J. Chem. Phys.* **1984**, *80*, 1050.
(19) Tsuboi, M.; Hirakawa, A. Y. *J. Mol. Spectrosc.* **1975**, *56*, 146.
(20) (a) Takeuchi, H.; Harada, I. *Spectrochim. Acta* **1986**, *42A(9)*, 1078. (b) Harada, I.; Takeuchi, H. In *Advances in Spectroscopy: Biological Systems*; Clarke, R. J. H., Hester, R. E., Eds.; Wiley, New York, in press.
(21) Song, P. S.; Kurtin, W. E. *J. Am. Chem. Soc.* **1969**, *91*, 4892.
(22) Auer, H. E. *J. Am. Chem. Soc.* **1973**, *95*, 3002.
(23) Walton, A. G. *Polypeptides and Protein Structure*; Elsevier: New York, 1981; p 165.

and may simply reflect the ratio of the *C* and *B* vibronic terms.

4. Trp also shows L_a-resonant vibronic activity for ν_{8a}- and ν_{8b}-like modes. The strong 220-nm absorption band, identified with the B_b transition, enhances ν_{8a} but not ν_{8b}, consistent with the near-long axis polarization calculated for the transition and the antisymmetric character of ν_{8b}. Strongest enhancement is seen for indole ring modes having substantial pyrrole ring character. These modes are enhanced only weakly in the short-wavelength (~195 nm) band, attributed to B_a, which selects for the ν_{8a} and ν_{8b} modes. B_a is suggested to be localized largely on the benzene ring, while B_b is a more delocalized transition.

Acknowledgment. We thank Chang Su for checking intensity measurements. This work was supported by NSF Grant CHE81-06084 and NIH Grant GM 25158. Very helpful conversations with Drs. A. C. Albrecht, L. D. Ziegler, and R. P. Rava are gratefully acknowledged.

Registry No. H-Phe-OH, 63-91-2; H-Tyr-OH, 60-18-4; H-Trp-OH, 73-22-3; PhOH, 108-95-2; PhOH·Na, 139-02-6; H-Tyr-OH·2Na, 69847-45-6.

Spin Distributions and Geometries of the Radical Cations of Sesquinorbornenes and Other Polycyclic Tetraalkylethenes

Fabian Gerson,*,† Georg Gescheidt,† Stephen F. Nelsen,*,‡ Leo A. Paquette,§ Mark F. Teasley,‡ and Liladhar Waykole§

Contribution from the Institut für Physikalische Chemie der Universität Basel, Klingelbergstrasse 80, CH-4056 Basel, Switzerland, the S. M. McElvain Laboratories of Organic Chemistry, Department of Chemistry, University of Wisconsin, Madison, Wisconsin 53706, and the Evans Chemical Laboratories, The Ohio State University, Columbus, Ohio 43210. *Received November 25, 1988*

Abstract: The radical cations of *anti*- and *syn*-sesquinorbornenes (**1** and **2**, respectively) and *syn*-sesquinorbornatriene (**4**) have been characterized by their hyperfine data. The proton coupling constants, in millitesla, are as follows: $\mathbf{1}^{\bullet+}$, 1.346 (2 γ-*anti*-H), 0.326 (4 β-H), 0.311 (4 γ-*exo*-H), 0.103 (2 γ-*syn*-H), and 0.068 (4 γ-*endo*-H); $\mathbf{2}^{\bullet+}$, 0.746 (2 γ-*anti*-H), 0.392 (4 β-H), 0.353 (4 γ-*exo*-H), 0.083 (2 γ-*syn*-H), and 0.076 (4 γ-*endo*-H); $\mathbf{4}^{\bullet+}$, 1.066 (2 γ-*anti*-H), 0.252 (4 β-H), 0.090 (2 γ-*syn*-H), and 0.064 (4 vinylic H). Hyperfine data are also reported for the radical cations of isopropylideneadamantane (**6**), sesquihomoadamantene (**7**), and dimethylhomoadamantene (**8**). Spin delocalization into the polycyclic alkyl groups is discussed, as well as the geometry of $\mathbf{1}^{\bullet+}$, $\mathbf{2}^{\bullet+}$, and $\mathbf{4}^{\bullet+}$. Comparison of the vertical ionization potentials in gas phase with oxidation potentials $E^{\circ\prime}$ in solution indicates that **1** and **2** have comparable relaxation energies.

Several derivatives of *anti*-sesquinorbornene (**1**) have a nearly planar geometry at the two olefinic carbons, as do ethenes with less constrained C=C—C bond angles. According to X-ray crystallography, the internorbornene dihedral angle 180 − φ is 177.9° or more (i.e., out-of-plane deformation φ = 2.1° or less) for **1A**[1] and five similar adducts having *syn*-alkyl groups at C(7)

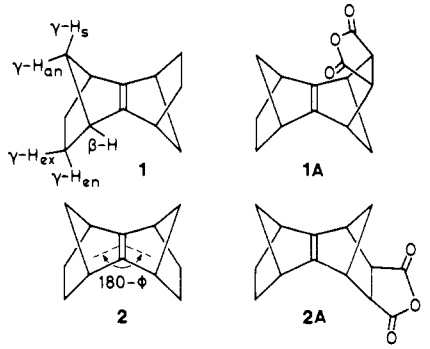

of the substituted norbornene moiety.[2] However, bending must be rather easy at the olefinic carbon atoms of **1**, since φ values of 13.2° have been determined by X-ray crystallography for its *exo*-4-nitrophenylmaleimide and *N*-methyltriazolinedione adducts.[3] Derivatives of *syn*-sesquinorbornene (**2**) are generally more bent; **2A**[1] and five similar adducts[1,2,4] all exhibit angles φ of 15.5–18°. Even larger values of φ have been found for derivatives of **2** having additional unsaturated bonds, 22.1° for **2B**[5] and 21.8° for **2C**.[6]

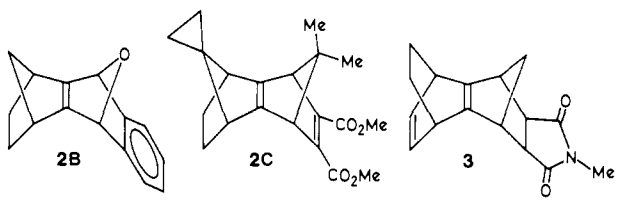

It has also been shown that the C=C—C angle restriction at the junction of the two norbornene moieties in **2** is not necessary for producing substantial φ values in derivatives of fused norbornenes. Thus **3** has φ = 11.8°,[7] four compounds with bicyclo[3.2.1] frameworks fused syn at the norbornene moiety exhibit φ values in the range 9.3–11.8°,[8] and several compounds with monocyclic

† Universität Basel.
‡ University of Wisconsin.
§ The Ohio State University.

(1) Watson, W. H.; Galloy, J.; Bartlett, P. D.; Roof, A. A. M. *J. Am. Chem. Soc.* **1981**, *103*, 2022.
(2) (a) Paquette, L. A.; Charumilind, P.; Böhm, M. C.; Gleiter, R.; Bass, L. S.; Clardy, J. *J. Am. Chem. Soc.* **1983**, *105*, 3136. (b) Paquette, L. A.; Hayes, P. C.; Charumilind, P.; Böhm, M. C.; Gleiter, R.; Blount, J. F. *Ibid.* **1983**, *105*, 3148.
(3) (a) Ermer, O.; Bödecker, C. D. *Helv. Chim. Acta* **1983**, *66*, 943. (b) Paquette, L. A.; Green, K. E.; Hsu, L.-Y. *J. Org. Chem.* **1984**, *49*, 3650.
(4) Hagenbuch, J. P.; Vogel, P.; Pinkerton, A. A.; Schwarzenbach, D. *Helv. Chim. Acta* **1981**, *64*, 1818.
(5) Bartlett, P. D.; Combs, G. L., Jr. *J. Org. Chem.* **1984**, *49*, 625.
(6) Paquette, L. A.; Green, K. E.; Gleiter, R.; Schaefer, W.; Gallucci, J. C. *J. Am. Chem. Soc.* **1984**, *106*, 8232.
(7) Paquette, L. A.; Carr, R. V. C.; Charumilind, P.; Blount, J. F. *J. Org. Chem.* **1980**, *45*, 4922.

0002-7863/89/1511-5518$01.50/0 © 1989 American Chemical Society